Journal of Sustainability Science and Management
Volume 17 Number 2, February 2022: 77-90
eISSN: 2672-7226

RAW WATER TREATMENT FROM SELECTED AREAS IN KELANTAN USING COCONUT SHELL DERIVED NANOMAGNETIC ADSORBENT COMPOSITE (CS-NMAC)

HUDA AWANG[1], PALSAN SANNASI ABDULLAH[1]*, LIM KAI WEN[1], HO YOON LING[1], JAYANTHI BARASARATHI[2], AND SITI NUURUL HUDA MOHAMMAD AZMIN[1]

[1]Faculty of Agro-Based Industry, Universiti Malaysia Kelantan, Jeli Campus, 17600 Jeli Kelantan, Malaysia. [2]Faculty of Health and Life Sciences, Inti International University Nilai, Negeri Sembilan, Malaysia.

**Corresponding author: palsan.abdullah@umk.edu.my*
Submitted final draft: 1 August 2021 *Accepted: 14 August 2021* http://doi.org/10.46754/jssm.2022.02.008

Abstract: The availability of clean water is a longstanding problem in the state of Kelantan, causing consumers to use alternative sources of raw water, such as rivers and groundwater. However, the quality of alternative sources of raw water is a concern due to turbidity problem. This research aims to develop a coconut shell derived nanomagnetic adsorbent composite (CS-NMAC) to purify contaminated raw water collected from Tanah Merah, Pasir Mas, and Jeli, in Kelantan. In this work, comparisons between the synthesized CS-NMAC and a commercial activated carbon (AC) revealed that the pore number for the CS-NMAC is f 43.3% higher than AC, while the presence of Fe-O peak at 536.98 cm-1 affirms the presence of magnetic properties on the surface of CS-NMAC. The maximum uptake capacity (Qmax) of CS-NMAC (3.79 mg/g) is higher than AC (1.76 mg/g). The purification of raw water sample at 200 rpm, 37 minutes, 27°C, and 0.04 g of CS-NMAC removed 94.26% of turbidity while Cd, Pb, Fe, Mn, and Hg were purified as following sorption capacity: 0.047, 0.02, 14.87, 0.4, and 0.004 mg/g respectively. These findings support CS-NMAC as a potent solution for improving access to clean treated water from alternative water sources.

Keywords: Groundwater, Kelantan, nanomagnetic, turbidity, water.
Abbreviations: [CS-NMAC, AC].

Introduction

Provision of safe treated water is a challenge in Kelantan. According to the 2015 audit report, water treatment plants operated by Air Kelantan Sendirian Berhad (AKSB) violated treated water quality criteria due to leakage of main and distribution pipes (National Audit Department, 2015). Most of pipelines in Kelantan are mild-steel pipes that are vulnerable to corrosion and cause heavy metal (iron and manganese) contamination in the supplied water (Ab Razak *et al*., 2016). As a result, most people in the northern part of Kelantan use alternative sources of water, such as river and groundwate, for daily consumption (Hayati *et al*., 2020). However, consumers of alternative water sources face poor water quality especially during the northeast monsoon season (October to March). The heavy downpour during the monsoon causes riverbank erosion, thus contaminating riverine water (Arif *et al*., 2019). The surface runoff carries contaminants into the water aquifer, including groundwater. In flood-affected areas, the situation will worsen. As a result, consumers of alternative water sources face difficulties in obtaining a regular supply of clean water throughout the year, potentially exposing them to waterborne illnesses (Nayan *et al*., 2018).

According to a preliminary survey, people in Tanah Merah, Pasir Mas, and Jeli think that groundwater obtained from a tube well does not have contamination problem. However, laboratory test revealed that turbidity reading (>5 NTU) of samples from tube well exceeded the Drinking Water Quality Standard (Minister of Health, 2012; Huda *et al*., 2020). The contaminants in raw water comprise of heavy metals and organic matter. Turbidity of water occurs due to the presence of suspended particles in water that could originate from various sources such as organic or inorganic matter, clay and silt (Gwenzy *et al*., 2017). The

challenging part in purifying turbidity in raw water of alternative water sources is the large amount of mud. High turbidity might lead to overloading of the coagulation – sedimentation filtration unit and increment of back-washing (Lo *et al.,* 2014).

One of the solutions to the problem is the Fenton process. The process requires reactions between aqueous mixture of ferrous ion (II) and hydrogen peroxide. The activated carbon plays vital roles in providing reactive surface area for adsorption with the Fenton process – supporting H_2O_2 electrogeneration and activation during adsorption simultaneously. A previous report by Apriani *et al.* (2016) revealed that the Fenton process purified turbidity in peat water efficiently (99%). However, the safety of water for consumption through this method is questionable. The heavy metal contaminants, especially iron, might enhance oxidative stress during the Fenton process and overproduce carcinogenic reactive oxygen species (Kicinski *et al.,* 2020).

Therefore, adsorption technique without additional chemical reaction is adopted in this study. A carbon-based adsorbent composite was used in the study due to its efficiency and ease of handling. This water treatment option was proposed in line with the 11th Malaysia Plan, which called for expanded use of alternative water sources by altering the systems to match local requirements (Economic Planning Unit, 2016). Activated carbon is a porous and carbon rich material produced via thermal conversion of biomass material and widely applied for various purposes, including adsorption for water treatment (Gwenzy *et al*., 2017). However, the activated carbon its disadvantages, like its difficulty to separate spent material from the liquid (Anyika *et al*., 2017).

Innovation of carbon-composites with magnetic properties through the incorporation of metal (iron) oxides into carbon material have been introduced (Anyika *et al*., 2017). The magnetization process can be achieved by use of ferric chloride ($FeCl_3$) and ferrous chloride ($FeCl_2$), among others. Magnetic carbon material has high adsorption capability as opposed to nonmagnetic carbon material. The magnetic characteristic can improve the effectiveness of separation and filtration process by magnetic force (Zubrik *et al*., 2014). Hence, magnetic carbon composites in aqueous solution can be separated by the presence of external magnetic field.

Besides successful removal of cadmium and methylene blue in wastewater, it is found that the adsorption reaction by magnetic biochar with mangosteen peels is insignificant and slows as time progresses (Ruthiraan *et al*., 2017). Such phenomenon occurred due to limited active sites on the surface to adsorb. Later, ultrafine magnetic activated carbon was introduced by Meng *et al.* (2019) to remove perfluorinated compounds in wastewater. The study showed that smaller sized adsorbent material displayed higher adsorption capacity due to large surface area, albeit unstable bond between Fe_3O_4 and ultrafine activated carbon (Meng *et al.,* 2019). In fact, the particles of magnetic material tend to form large aggregates when interacting with each other. Therefore, the idea of synthesizing nano-sized adsorbent is to improve surface area for adsorption and stability of the compound (Liu *et al*., 2020).

There are a few types of iron oxide nanoparticles, such as FeO (wÜstite), ϒ-Fe_2O_3 (maghemite) and Fe_3O_4 (magnetite), commonly used for environmental engineering purposes (Lo *et al*., 2014). The quantum mechanical property of electron spin has a vital role for magnetism. Most of the outer shell electrons in the bulk material are occupied in bonding pairs and later, became non-magnetic. Reduction of electron coordination with nanoscale magnetic structure will provide more available electrons for magnetism, therefore, providing greater propensity of magnetic behavior (Wannahari *et al*., 2018). Apart from that, the nano-sized iron oxide materials immobilized on organic and inorganic support can prevent aggregation (Liu *et al.*, 2020). Due to such phenomenon, an innovation by incorporating nanomagnetic property onto activated carbon or biochar

is introduced to improve performance of adsorption (Wannahari *et al*., 2018).

This study aims to synthesize and characterize coconut shell derived nanomagnetic adsorbent composite (CS-NMAC) and evaluate the efficiency in turbidity reduction and heavy metals (Al, As, Cd, Cu, Pb, Mg, Mn, Hg, Se, Ag, Fe, Cr, Zn, Na, B, and Ba) removal from raw water of alternative water sources. The challenge was to ensure that the performance of the lab-developed coconut shell derived nanomagnetic adsorbent composite (CS-NMAC) is competitive to commercial activated carbon (AC).

Materials and Methods

All the reagents used are of analytical grade; this consisted of potassium hydroxide (KOH), hydrochloric acid (HCl), nitric acid (HNO_3), iron (III) chloride hexahydrate ($FeCl_3.6H_2O$), iron (II) sulphate heptahydrate ($FeSO_4.7H_2O$), ammonium hydroxide ($NH_3.H_2O$), epichlorohydrin, and ethanol.

Carbonization and Activation of Coconut Shell (CS)

Coconut shell (CS) was carbonized using a modified drum carbonization method. The carbonized CS were ground into powder and then subjected to activation with KOH at a ratio of 1:3, with slow agitation. The mixture was left to mature for about 5 to 6 h and filtered before rinsing off with ddH_2O. The powder was dried in oven (90°C -100°C). The dried powder was placed in a muffle furnace (Carbolite ELF 11/6B) and heated to 800-900°C (10°C/min), and kept for 15-30 minutes. The cooled down activated coconut shell (ACS) powder was washed, neutralized with 5% HCl, dried and stored for further modification.

Synthesis of Coconut Shell Derived Nanomagnetic Adsorbent Composite (CS-NMAC)

The synthesis of coconut shell derived nanomagnetic adsorbent composite (CS-NMAC) was initiated by acclimatizing ACS powder with nitric acid (HNO_3) solution for 1 h at 80°C following the method previously described by Wannahari *et al*. (2018). This was to remove any impurities and enhance the active surface sites of the carbon particle. At the same time, $FeCl_3.6H_2O$ and $FeSO_4.7H_2O$ were dissolved with 450 mL of deionized water under mechanical stirring for 30 minutes at 30°C. The chemical precipitation was achieved under vigorous stirring by adding 30-60 mL of ammonium hydroxide ($NH_3.H_2O$) solution. The reaction vessel was kept at 70°C for 1 h. Five grams of ACS powder was added and mixed completely using mechanical stirring. Afterwards, 6 mL of epichlorohydrin was added and stirred at 85°C for 1 hour. The reaction mixture was then sonicated (Q Sonica) at 80 λ for 1 hour. The mixture was continuously stirred for another hour at 85°C. The mixture was then cooled down to room temperature. The precipitate was washed rapidly with deionized water and ethanol, and dried at 50°C for 24-48 hour.

The dried CS-NMAC were sieved into their respective particle size ranges (45-300 μm). The sieved samples were washed with water to remove impurities and filtered by using Fisher brand filter paper (No. 2). The washing was considered as complete when the filtrate appeared clear and the pH value of filtrate approached pH 7. The washed samples were dried in the oven at 80°C for 3 to 5 days depending on the progress of drying. The dry CS-NMAC powder were then stored in containers according to their particle size range for further testing and characterization.

Characterization of CS-NMAC

The newly synthesized CS-NMAC was subjected to characterization and AC was used as the reference for comparison. Proximate analyses were carried out for the estimation of volatile matter, moisture, ash, and fixed carbon content of the respective adsorbents (Milne *et al*., 1992). The iodine number value determination was carried out by the protocol provided by ASTM (2003). The FTIR analysis was conducted

using iZ10 FT-IR Spectrometer (Thermo Fisher Scientific, USA) with spectral ranges from 400 - 4000 cm^{-1} to identify the functional groups in the samples. The surface morphology of the samples was observed through SEM by using JSM-IT200LV (JOEL Ltd, Tokyo, Japan) with a 15 kV accelerating voltage.

Adsorption Studies

The obtained water sample was used to investigate the adsorption of CS-NMAC and AC. The data was plotted according to Langmuir and Freundlich isotherm equation.

The experiments were carried out by batch method and uptake of turbidity by the adsorbent was calculated using Equation 1:

$$qe = \frac{(Ci-Ce)v}{w} \quad (1)$$

Where qe is uptake capacity (mg/g), Ci and Ce are the initial and equilibrium concentration (mg/L), v is working volume (L), and w is weight of the adsorbent (g).

Langmuir isotherm considers the surface coverage for adsorbate-adsorbent interaction. The equation for Langmuir isotherm is as follows (Equation 2):

$$\frac{1}{qe} = \frac{1}{qmKL}\left(\frac{1}{Ce}\right) + \frac{1}{qm} \quad (2)$$

Where qe is uptake capacity (mg/g), qm is the maximum uptake capacity (mg/g), K_L is Langmuir constant (mg/g), and Ce is equilibrium concentration of adsorbate (mg/g).

R_L is a dimensionless constant factor in Langmuir isotherm. The equation for expression of R_L is as follows (Equation 3):

$$RL = \frac{1}{(1+KLCi)} \quad (3)$$

Where, C_i is the initial concentration of the raw water of alternative water sources. The R_L is an indication of the shape of the isotherm based on the obtained value, the indication as follows: $R_L > 1$ unfavorable, $R_L = 1$ linear, $0 < R_L < 1$ favorable, and $R_L = 0$ irreversible.

Freundlich isotherm postulates that the adsorption process occurs on heterogeneous surfaces. The expressed equation is to determine heterogeneity and distribution active sites of the surface. The equation of Freundlich isotherm is as follows (Equation 4):

$$log\ log\ qe = log\ log\ kf + \frac{1}{n}\ (log\ log\ Ce) \quad (4)$$

Where kf is adsorption capacity (L/mg) and $1/n$ is adsorption intensity.

Water Sampling and Testing

The water samples were collected from selected areas in the districts of Tanah Merah, Pasir Mas, and Jeli in Kelantan (Table 1). The districts were selected based on previous questionnaire responses.

Table 1: Water sample collection

Sample	Coordinate of Location	District	Sources of Water
S1	N 5° 48 56.8 E 102° 0757.1	Tanah Merah	Well
S2	N 5° 50 35.3 E 102° 0728.0	Tanah Merah	Tube Well
S3	N 5° 49 31.7 E 102° 0736.2	Tanah Merah	Well
S4	N 6° 03 08.6 E 102° 0639.6	Pasir Mas	Well
S5	N 6° 03 09.2 E 102° 0639.5	Pasir Mas	Well
S6	N 6° 02 30.6 E 102° 0755.2	Pasir Mas	Well
S7	N 5° 76 66.7 E 101° 8681.0	Jeli	River
S8	N 5° 76 16.4 E 101° 8624.5	Jeli	River
S9	N 5° 45 42.1 E 101° 5149.6	Jeli	River

Water Purification and Analysis

The raw water samples (S1, S2, S3, S4, S5, S6, S7, S8, and S9) were combined to reflect the treatment approach which will cater to water from all sources. Batch adsorption was carried out with 10% (w/v) adsorbent with agitation at 200 rpm for 37 minutes to purify the combined raw water sample. The samples were tested for initial water turbidity reading, pH, heavy metals (As, Cd, Cu, Pb, Mg, Mn, Se, Ag, Fe, Cr, Zn, Na, B, and Ba), and bacterial count coliform count and *Eschericia coli* count had been conducted.

Results and Discussion

Table 2 shows that both CS-NMAC and AC have high levels of fixed carbon (~98%). However, CS-NMAC has higher iodine number (732.95 mg/g) relative to AC. This reflects that CS-NMAC has larger carbon surface and higher porosity compared to AC (Sewu *et al*., 2017). In addition, AC contains a higher content of ash compared to CS-NMAC. The ash contains inorganic residues that may block pores and lead to a decrease in surface area for adsorption (Ahmad *et al*., 2014).

FTIR was performed to detect functional groups present on the surface of CS-NMACand AC. Figure 1 depicts the saturated alkene (C=C) stretching on the surface of CS-NMAC (1651.69 cm^{-1}) and AC (1567.89, 1645.28, and 2082.08 cm^{-1}). Furthermore, ketone stretching (C=O) was discovered on CS-NMAC (1732.14 and 1875.6 cm^{-1}) and (1682.48, 1694.65, and 1732.2 cm^{-1}). This observation was also consistent with previous findings that showed peaks at 1700 cm^{-1} (Ruthiraan *et al*., 2017) and 1689 cm^{-1} (Santosh *et al*., 2020) to be ketones. The pyrolysis process is responsible for the formation of a ketone functional group on the surface of CS-NMAC and AC (Ruthiraan *et al.,* 2017). The hydroxyl group (-OH-) on the surface of CS-NMAC (3667.52, and 3646.24 cm^{-1}) and AC (3646.26, 3673.78, and 3667.81 cm^{-1}) is consistent with Cheng *et al.* (2019), who proposed that the hydroxyl group (3600 cm^{-1}) plays an important

Table 2: Proximate analysis for CS-NMAC and AC

Types of Adsorbents	Moisture (%)	Volatile matter (%)	Ash (%)	Fixed carbon (%)	Iodine number (mg/g)
CS-NMAC	3.70	40.90	62.46	98.93	732.95
AC	2.80	48.61	72.25	98.76	511.15

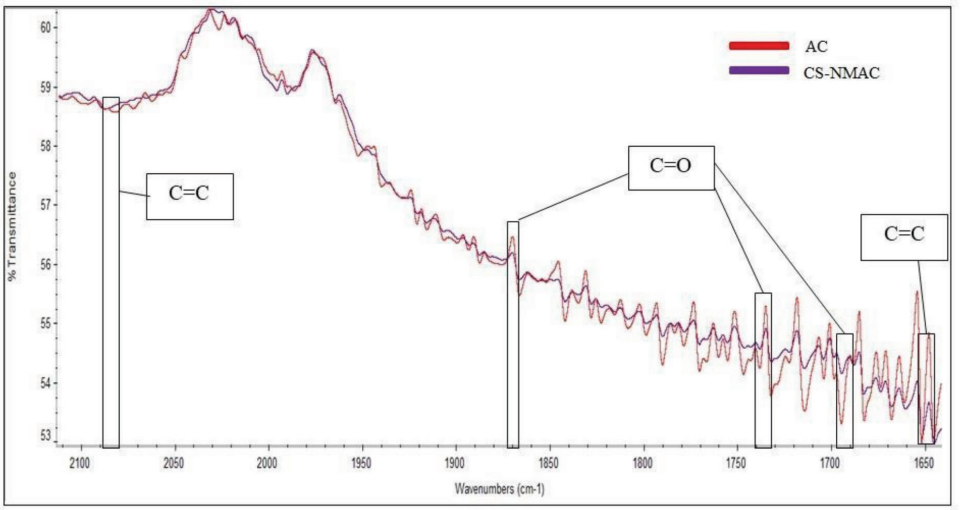

Figure 1: The C=O and C=C group of AC and CS-NMAC in FTIR spectra at 1650-2100 cm^{-1}

role in the adsorption mechanism. The C-H group was found on the surface of CS-NMAC (807.5 cm^{-1}) and AC (1471.05 cm^{-1}). The appearance of absorption at peaks 700-900 cm^{-1} attributed to CH in out-of-plane bending in the edges of aromatic rings confirms the presence of carbon-derived properties in the adsorbents (Eltaweil *et al.,* 2020). The comparison between AC and CS-NMAC is absorption at 536.98 cm^{-1} attributed to the presence of Fe-O iron oxide. The current findings appear to be encouraging when compared to Rajan *et al.* (2019), with Fe-O absorption at 538.9 cm^{-1}. As a result, Fe-O confirms the presence of hematite (Fe_3O_4) in modified biocarbon (Ruthiraan *et al.,* 2017).

X-Ray diffraction (XRD) patterns of CS-NMAC and AC are shown in Figure 2 (a) and (b), respectively. The analysis revealed that both materials were present as a crystalline solid, has well-defined edges and faces, and the atoms are periodically arranged in a 3D space. In the analysis, X-rays were scattered in certain directions when they hit the formed lattice planes to form well-resolved X-ray diffraction patterns (LibreTexts, 2019).

Based on Figure 2(a) the crystalline phase of CS-NMAC is related to the peak at 2θ = 18.321º, 30.139º, 35.339º, 37.041º, 43.091º, 47.156º, 53.396º, 56.989º, 62.567º, 65.781º, 70.981º, 74.006º, 75.046º, 79.017º, 81.948º, 86.769º and 89.700º, suggesting the presence of Fe_3O_4 in CS-NMAC (Wannahari *et al*., 2018; Balaji *et al*., 2009). The intense peaks seen at 2θ values of 36.095º, 41.862º, 60.676º, 72.683º and 76.464º were assigned as FeO. The Fe_2O_3 peak attributes were identified at 30.321º, 34.001º, 35.732º, 37.368º, 38.955º, 40.494º, 43.429º and 46.194º. According to elemental analysis, iron (72.2%) was the major element present in CS-NMAC followed by oxygen (27.8%). This confirmed that CS-NMAC was coated and incorporated with iron magnetic nano particles to exhibit unique properties, which include superparamagnetic, greater surface area for easier separation methodology (Wannahari *et al*., 2018; Ali *et al*., 2016).

Meanwhile, based on Figure 2 (b) the crystalline phase of AC was related to the peak observed at 2θ = 21.81º, 22.26º, 25.45º, 28.36º, 43.10º, 44.70º, 47.36º, 48.42º, 52.16º, 52.80º, 57.24º, 77.03º and 82.10º, indicating the appearance of SiO_2. Five peaks at 2θ values of 26.54º, 42.42º, 44.70º, 59.74º and 87.55º were identified to belong to graphite. The analysis depicts the major elements found in AC is, SiO_2 (52.2%) and graphite (47.8%).

Thus, different diffractograms observed between CS-NMAC and AC at peak 2θ range of 27 º to 47 º suggested the changes of crystallinity on the materials resulting from the formation of iron oxide nanoparticles on CS-NMAC.

Scanning electron microscope (SEM) image of granular CS-NMAC and AC are presented in Figure 3(a) and 3(b), respectively. SEM analysis showed clear images of granular CS-NMAC and porous AC.

The thermodynamic equilibrium models fitted with experimental data by Langmuir (1/*Qe*vs 1/*Ce*) and Freundlich isotherm (log *Qe* vs log *Ce*) models for CS-NMAC and AC are shown in Figure 4. The estimated values of Langmuir and Freundlich isotherm constants are presented in Table 3. According to the obtained Langmuir isotherm constant, maximum adsorption (Qmax) by CS-NMAC (3.791 mg/g) is higher as compared to AC (1.755 mg/g). The given R_L for CS-NMAC and AC are within the range $0 < R_L < 1$, so the models for both adsorbents are favorable. Generally, the Langmuir isotherm showed the best fit model with R^2 for CS-NMAC (0.994) and AC (0.971). This indicates the turbidity reduction by means of adsorption occurred on a homogenous adsorbent surface. Apart from that, the kf is constant for the Freundlich isotherm to determine adsorption capacity. So, based on Table 3, kf value for CS-NMAC (14.938 mg/g) is higher than AC (0.7187 mg/g). Meanwhile the 1/n were found to be 0.9608 (CS-NMAC) and 0.2094 (AC), indicating it is a normal adsorption. The comparisons of maximum adsorption capacity of CS-NMAC with other adsorbents are shown in Table 4.

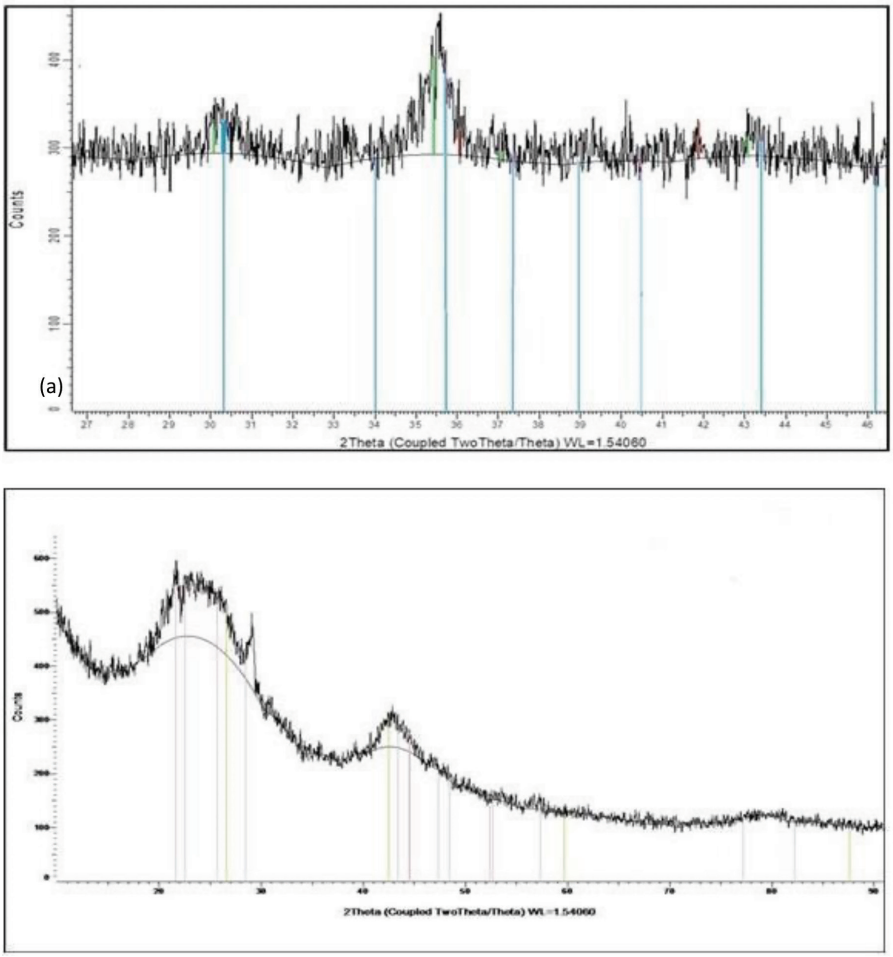

Figure 2: XRD patterns of (a) CS-NMAC and (b) AC

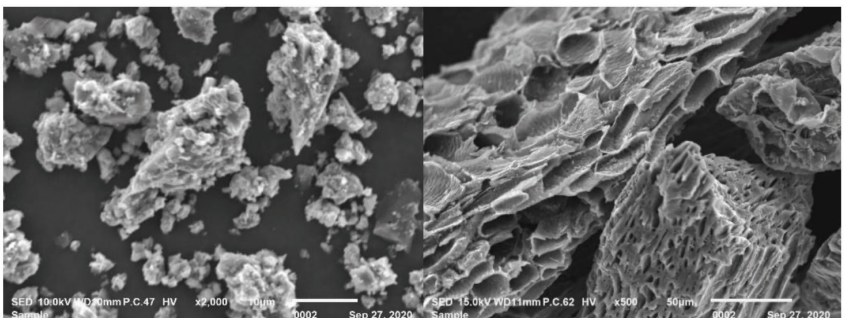

(a) (b)

Figure 3: Scanning electron microscopy images for (a) CS-NMAC and (b) AC

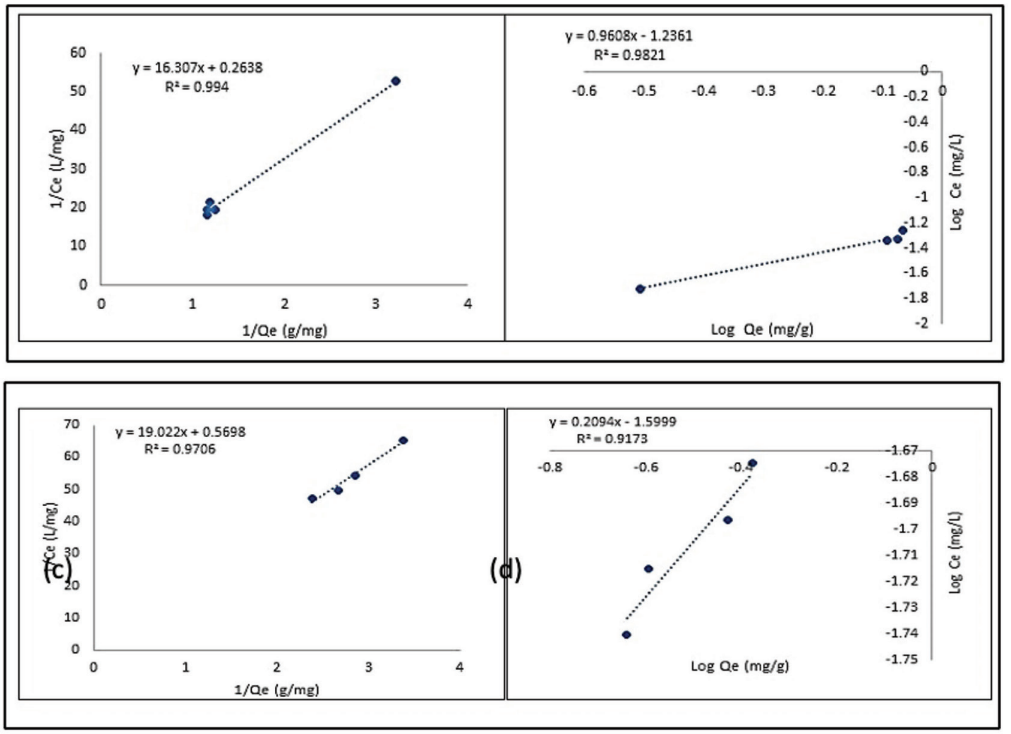

Figure 4: Isotherm models fitted to the experimental turbidity removal data. (a) Langmuir isotherm model (CS-NMAC), (b) Freundlich isotherm model (CS-NMAC), (c) Langmuir isotherm (AC), and (d) Freundlich isotherm (AC)

Table 3: Isotherm constant values obtained from fitting Langmuir and Freundlich isotherm models for CS-NMAC and AC

Types of Isotherm Models	Parameters	Types of Adsorbents	
		CS-NMAC	AC
Langmuir Isotherm	Q_{max} (mg/g)	3.791	1.755
	R_L (L/mg)	0.968	0.989
	K_L (L/mg)	0.061	0.0.30
	R^2	0.994	0.971
Freundlich Isotherm	k_f (mg/g)	14.938	0.7187
	n	1.041	4.776
	1/n(L/mg)	0.9608	0.2094
	R^2	0.9821	0.9173

Table 5 displays the water quality analysis before and after purification using CS-NMAC of water collected from selected areas of Kelantan. Comparison with local standards of Malaysia Food Act 1983 revealed that some of the parameter readings are above the allowable limit. The turbidity of the water is 18 times higher than the permissible limit. Turbidity may occur due to heavy rainfall, excessive extraction of groundwater, fissures within the

Table 4: Comparisons of adsorption capacities for removal of organic contaminants with other adsorbents

Adsorbents	Contaminants	Types of Isotherm	Q_{max} (mg/g)	References
TiO_2 nanoparticles	Dissolved organic carbon	Freundlich	3.7	Gora *et al.,* 2017
Magnetite	Humic acid	Langmuir	2.6	Wongcharee *et al.*, 2019
Granular activated carbon	Dissolved natural organic matter	Freundlich	2.4	Sari et al., 2021
CS-NMAC	Water turbidity	Langmuir	3.76	This study

Table 5: Water quality analysis

Parameter	Result		Standard (Malaysian Food Act 1983)	Unit
	Before purification	After purification		
pH	6.39	5.80	6.5-8.5	-
Turbidity	36.80	2.18	2.000	FAU
Total chlorine	0.08	0.03	<0.2	mg/L
Arsenic	<0.005	<0.01	0.010	mg/L
Cadmium	<0.05	< 0.1	0.003	mg/L
Copper	0.14	< 0.1	1.000	mg/L
Lead (as Pb)	0.03	< 0.1	0.010	ppm
Magnesium	2.01	0.52	150.000	ppm
Manganese	0.50	< 0.1	0.100	ppm
Mercury	<0.005	<0.001	0.001	ppm
Selenium	<0.005	< 0.1	0.010	ppm
Silver	<0.01	<0.1	0.050	ppm
Total Iron	14.97	<0.1	0.300	ppm
Chromium	0.02	<0.1	0.050	ppm
Zinc	0.24	< 0.1	3.000	ppm
Sodium	3.87	4.35	200.000	ppm
Boron	<0.01	<0.1	0.500	ppm
Barium	0.09	< 0.1	0.700	ppm
Coliform count	$1.4x10^5$	< 1	ND	MPN/100 ml
Escherichia coli count	<1.8	<1	ND	MPN/100 ml

*FAU = Formazin Attenuation Uni *ND = Not Detected

aquifer, and fecal pollution of shallow domestic wells (Stevenson & Bravo, 2019; Diaz-Alcaide *et al*., 2019). Heavy rainfall will leach into the soil in agricultural areas into the nearby rivers (Stevenson & Bravo, 2019). The possible reason for the groundwater to be turbid could also be related to high amounts of iron in the water. This postulation is supported by a study by

Harun *et al*. (2019) who also reported increase in the water turbidity due to high amount of iron present in the groundwater. Table 5 shows that the turbidity in raw water was purified with 94.8% removal efficiency using CS-NMAC. Lo *et al.* (2020) also reported that the application of magnetic aggregation and separation process reduced turbidity of various sources of raw water significantly.

Over the last few decades, the people living in Jeli, Tanah Merah, and Pasir Mas were using land for agricultural activities extensively, hence accumulating chloride ions from fertilizers and manure in the soil. The infiltrated rainfall will flush the accumulated chloride ions into nearby water sources (Salem *et al.,* 2018). In addition to that, water samples were collected from rural area (Jeli) and outskirt areas (Tanah Merah and Pasir Mas) where known for agricultural activities. The agricultural activities released fertilizers, animal feed and animal waste. So, based on the obtained result (Table 5) the CS-NMAC removed 62.5% total chlorine in the water sample.

The presence of heavy metals in alternative water sources compromise human health, causing symptoms such as nausea, vomiting, headache, skin irritation, and long-term or chronic exposure may leads to anemia, kidney damage, and cancer due to toxic properties in the heavy metals (Jayanthi *et al*., 2017). The characterization of heavy metal from the raw water of alternative water sources analysis (Table 5) indicates the presence of Cd, Pb, Mn, Fe and Hg violated the Malaysia Food Act 1983 standard limit that may be due to various anthropogenic activities around the water resources area. Application of nanomagnetic carbon composite for the removal of heavy metals has been reported by Mahmood *et al*. (2018) and Joshi *et al*. (2019). The sorption capacity of heavy metals observed after purification with CS-NMAC were as following; Cd (0.047 mg/g), Pb (0.02 mg/g), Mn (0.4 mg/g), Fe (14.87 mg/g) and Hg (0.004 mg/g). Although concentration of Mg and Zn in raw water did not exceed the limit in the prescribed standard, these heavy metal concentrations are reduced after adsorption with sorption capacity (1.49 mg/g) and 0.14 (mg/g) respectively. The adsorption of heavy metal ions by CS-NMAC involves ion exchange capacity on its surface. The mechanism involves chemical cross-linking between the heavy metal ions and the surface functional groups of the composites (Deng *et al*., 2017).

The gradual loss of ions from raw water is likely due to diffusion through micropores that govern incorporation of these ions into the surface of CS-NMAC. In addition to that, the iron oxide nano particles (FeOH) embedded on the surface of CS-adsorbent (Figure 5) is important in adsorption reaction.

Furthermore, it is proposed that a nucleation effect occurs on the aggregation (Figure 3 (a)) of FeOH through electron exchange to eliminate organic pollutants, such as turbidity in (Handler, 2009). The dispersed CS-NMAC in aqueous solution collide each other to form high-density magnetized flocs. Thus, the FeOH on the surface of CS-NMAC plays the role of a nucleus to form electrostatic interaction with suspended particles in turbid raw water of alternative water sources. Apart from that, Lo *et al.,* (2014) suggested low dispersitivity among CS-NMAC at solution (pH 6-6.4) due to low potential of iron oxide nanoparticles leading to formation of weak aggregation.

Besides, the nucleus effect is also involved in adsorption of heavy metals. During the adsorption reaction, the scavenging manganese ions from raw water of alternative water sources formed electrostatic interactions with FeOH, resulting in manganese dioxide precipitate on the surface of the CS-NMAC, as shown in Equation 5.

$$2Fe(OH)_2 + Mn \rightarrow MnO_2 + 2Fe + 2H_2O \quad (5)$$

Moreover, natural organic matter (NOM) comprises a matrix of organic substances. Hence, size of surface pores and functional groups have important roles in sequestering natural organic matter (NOM) from aqueous solution (Allgayer

et al., 2020). The NOM molecules are likely to diffuse into the pore of CS-NMAC. Besides, electrostatic attraction will occur if the surface of CS-NMAC and NOM have different charges.

Apart from that, another postulation regarding adsorption of organic contaminants is the pH of aqueous solution. If the alternative water source is more alkaline than the isoelectric point of the surface of CS-NMAC; a reaction as in Equation 6 will occur. Thus, ionic bonds will be formed between Fe^{2+} and Cl_2^- as in Equation 7.

$$FeOH \leftrightarrow FeO^- + H^+ \quad (6)$$

$$\mathbf{2}FeO + \mathbf{2}Cl_2 \rightarrow \mathbf{2}FeCl_2 + O_2 \quad (7)$$

Conclusion

In conclusion, based on the characterization analysis, the number of pores for CS-NMACis 43.39% higher than AC. In addition, the presence of FeO on the surface of CS-NMAC as observed at 536.98 cm^{-1} and crystalize phase at 2θ values 36.095º, 41.862º, 60.676º, 72.683º and 76.464º are important for verifying magnetic properties. The isotherm study shows that monolayer adsorption occurs in CS-NMAC and AC, while maximum uptake capacity (Qmanx) by CS-NMAC is the highest (3.791 mg/g). The purification of raw water collected from selected areas with CS-NMAC showed that the purified water complies the Standard Malaysian Food Act 1983. Hence, the development of coconut shell derived nanomagnetic adsorbent composite (CS-NMAC) is highly preferable to improve the quality of alternative water sources and fulfills the sustainable development goal ofclean water and sanitation for all.

Acknowledgements

The authors acknowledge financial support from Universiti Malaysia Kelantan Research Fund (R/SGJP/A07.00/01397A/005/2018/0057).

References

Ab Razak, N. H., Praveena, S. M., Aris, A. Z., & Hashim, Z. (2016). Quality of Kelantan drinking water & knowledge, attitude, & practice among the population of Pasir Mas, Malaysia. *Public Health*, *131*, 103-111.

Ahmad, M. A., Herawan, S. G., & Yusof, A. A. (2014). Effect of activation time on the

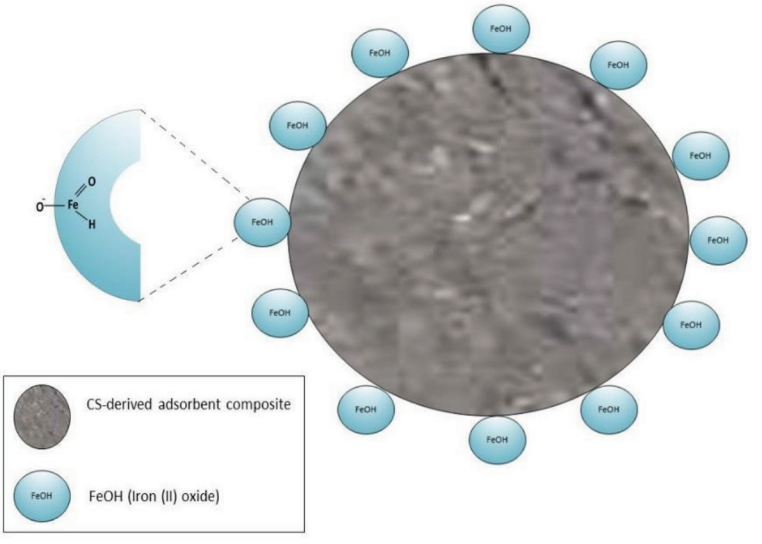

Figure 5. The surface matrix of CS-NMAC embedded with iron (II) oxide (FeOH) in an aqueous system

Pinang frond based activated carbon for Remazol Brilliant Blue R removal. *Journal of Mechanical Engineering & Sciences*, *7*(1), 1085-1093.

Ali, A., Hira, Z., Muhammad, Z., Ihsan, U. H., Abdul Rehman, P., Joham, S. A., & Altaf, H. (2016). Synthesis, characterization, applications, & challenges of iron oxide nanoparticles. *Nanotechnology, Science & Applications*, *9*, 49-67.

Allgayer, R., & Yousefi, N., Tufenkji, N. (2020). Graphene oxide sponge as adsorbent for organic contaminants: Comparison with granular activated carbon & influence of water chemistry. *Environmental Science Nano*, *7*, 2669-2680.

Anyika, C., Asri, N. A. M., Majid, Z. A., Yahya, A., & Jaafar, J. (2017). Synthesis & characterization of magnetic activated carbon developed from palm kernel shells. *Nanotechnology for Environmental Engineering*, *2*(1), 1-25.

Apriani, M., Masduqi, A., & Hadi, W. (2016). Degradation of organic, iron, color, & turbidity from peat water. *ARPN Journal of Engineering and Applied Science*, *11*(13), 26-29.

Arif, M. C. A. R., Aniruth, A., Shi, X., Liu, S., Masni, M. A., Wan Zuhairi, W. Y., & Che Abd Rahim, M. (2019). Distribution of Chromium and Gallium in the Total Suspended Solid & distribution of Chromium and Gallium in the Total Suspended Solid & Surface Sediments of Sungai Kelantan, Kelantan, Malaysia. *Sains Malaysiana*, *48*(11), 2343-2353.

ASTM E1755-01. Standard Method for the Determination of Ash in Biomass (2003). United States of America: American Society for Testing & Materials International.

Balaji, N., Begum, K. M. M. S., Anantharaman, N., & Uddin, M. S. (2009). Adsorption & desorption of L-Phenylalanine on nano-sized magnetic particles. *ARPN Journal of Engineering and Applied Sciences*, *4*(8), 39-44.

Cheng, H., Ai, J., Zhang, W., Fu, X., Du, Y., & Wang, D. (2019). Preparation of biological activated carbon (BAC) using aluminum salts conditioned sludge cake for the bio-refractory organic contaminants removal from anaerobically digested liquor. *Colloids & Surfaces A: Physicochemical and Engineering Aspects*, *561*, 89-100.

Deng, Y., Zhang, T., & Wang, Q. (2017). Biochar adsorption treatment for typical pollutants removal in livestock wastewater: A review. In W.-J. Huang (Ed.), *Engineering Applications of Biochar*. Rijeka: IntechOpen. https://doi.org/10.5772/intechopen.68253

Díaz-Alcaide, S., & Martínez-Santos, P. (2019). Mapping fecal pollution in rural groundwater supplies by means of artificial intelligence classifiers. *Journal of Hydrology*, *577*(June).

Economic Planning Unit. (2016). *Eleventh Malaysia Plan 2016-2020 Anchoring Growth on People*. Putrajaya: Percetakan Nasional Malaysia Berhad.

Eltaweil, A. S., Ali Mohamed, H., Abd El-Monaem, E. M., & El-Subruiti, G. M. (2020). Mesoporous magnetic biochar composite for enhanced adsorption of malachite green dye: Characterization, adsorption kinetics, thermodynamics & isotherms. *Advanced Powder Technology*, *31*(3), 1253-1263.

Gora, S., & Andrews, S. (2017). Adsorption of natural organic matter and disinfection byproduct precursors from surface water onto TiO2 nanoparticles: pH effects, isotherm modeling & implications for the use of TiO2 for drinking water treatment. *Chemosphere*, *174*, 363-370.

Gwenzi, W., Chaukura, N., Noubactep, C., &Mukome, F. N. D. (2017). Biochar-based water treatment systems as a potential low-cost and sustainable technology for clean water provision. *Journal of Environmental Management*, *197*, 732-749.

Handler, R. M. (2009). *Still oxides run deep: studying redox transformations involving Fe & Mn oxides using selective isotope techniques*. The University of Iowa.

Hayati N, H., Ismail, Y., & Raksmey, M. (2020). Comparison of applications to evaluate groundwater. *Geosciences*, *10*(289), 1-25.

Hazimah, H., Mohamad Roslan, M., Nurhidayu, S., Zulfa Hanan, A., & Faradiella, M. (2019). Hydrogeochemistry investigation on groundwater in Kuala Langat, Banting, Selangor. *Bulletin of the Geological Society of Malaysia*, *67*(June), 127-134.

Huda, A., Palsan, S. A., & ZulAriff, A. L. (2020). A preliminary study of local behaviour, perceptions & willingness to pay towards better water. In *IOP Conference Series: Earth and Environmental Science* (pp. 1-10).

Jayanthi, B., Emenike, C. U., Auta, S. H., Agamuthu, P., & Fauziah, S. H. (2017). Characterization of induced metal responses of bacteria isolates from active non-sanitary landfill in Malaysia. *International Biodeterioration & Biodegradation*, *119*, 467-475.

Joshi, S., Sharma, M., Kumari, A., & Shrestha, S. (2019). Applied sciences Arsenic Removal from water by adsorption onto Iron Oxide / Nano-Porous Carbon Magnetic Composite. *Applied Sciences*, *9*(3732), 1-12.

Kicinski, W., Dyjak, S. (2020). Transition metal impurities in carbon-based materials: Pitfalls, artifacts & deleterious effects. *Carbon*, *168*, 748-845.

Liu, Y., Yu, H., & Zou, D. (2020). One-Step synthesis of metal-modified nanomagnetic materials & their application in the removal of Chlortetracycline. *ACS Omega*, *5*(10), 5116-5125.

Lo, S., Wang, Y., & Hu, C. (2014). High turbidity reduction during the storm period by applied magnetic field. *Journal of Environmental Management*, *17*(5), 365-370.

Mahmood, T., Aslam, M., Naeem, A., Siddique, T., & Ud, S. (2018). Adsorption of as (III) from aqueous solution onto iron impregnated used tea activated carbon: Equilibrium, kinetic & thermodynamic study. *Journal of the Chilean Chemical Society*, *63*(1).

Meng, P., Fang, X., Maimaiti, A., Yu, G., & Deng, S. (2019). Efficient removal of perfluorinated compounds from water using a regenerable magnetic activated carbon. *Chemosphere*, *224*, 187-194.

Milne, T. A., Chum, H. L., Agbleyor, F. A., & Johnson, D. K. (1992). Standardized Analytical Methods. In *Biomass & Bioenergy. Proceedings of International Energy Agency Bioenergy Agreement Seminar* (pp. 341-366).

Ministry of Health (MOH). (2012). *Drinking Water Quality Standard*. http://kmam.moh.gov.my/public-user/drinking-water-quality-standard.html

National Audit Department. (2015). *National Auditor General Report 2015*. Putrajaya.

Nayan, N., Saleh, Y., Hashim, M., Mahat, H., & See, K. L. (2019). Investigating groundwater quality in the flood prone neighborhood area in Malaysia. *Indonesian Journal of Geography*, *51*(2), 123-130.

Ruthiraan, M., Abdullah, E. C., Mubarak, N. M., & Noraini, M. N. (2017). A promising route of magnetic based materials for removal of cadmium & methylene blue from wastewater. *Journal of Environmental Chemical Engineering*, *5*(2), 1447-1455.

Salem, M. N., Tarmizi, I., Kamal, A. (2018). Flood susceptibility assessment in Kelantan River basin using copula. *International Journal of Engineering & Technology*, *7*(2), 584-590.

Sari, B., Oztas, A. E., Keskinkan, O., & Ersu, C. B. (2021). Batch and continuous design of a full-scale treatment facility for removing dissolved natural organic matter. *Clean-Soil, Air, Water*, *49*, 1-20.

Sewu, D. D., Boakye, P., & Woo, S. H. (2017). Highly efficient adsorption of cationic dye by biochar produced with Korean cabbage waste. *Bioresource Technology*, *224*, 206-213.

Stevenson, M., & Bravo, C. (2019). Advanced turbidity prediction for operational water supply planning. *Decision Support Systems*, *119*(February), 72-84.

Wannahari, R., Sannasi, P., Nordin, M. F. M., & Mukhtar, H. (2018). Sugarcane bagasse derived nano magnetic adsorbent composite (SCB-NMAC) for removal of Cu^{2+} from aqueous solution. *ARPN Journal of Engineering and Applied Sciences*, *13*(1), 1-9.

Wongcharee, S., Aravinthan, V., & Erdei, L. (2019). Removal of natural organic matter & ammonia from dam water by enhanced coagulation combined with adsorption on powdered composite nano-adsorbent. *Environmental Technology & Innovation*, *17*(100557).

Zubrik, A., Lovas, M., Matik, M., Stefusova, K., &Hredzak, S. (2014). Synthesis of magnetic materials from natural carbon precursors – A review. *Journal of the Polish minuteseral Engineering Society*, 127-130.